Atomic layer deposited molybdenum oxide for the hole-selective contact of silicon solar cells

Available online at www.sciencedirect.com

ScienceDirect

Energy Procedia 92 (2016) 443 – 449

Energy Procedia

6th International Conference on Silicon Photovoltaics, SiliconPV 2016

Atomic layer deposited molybdenum oxide for the hole-selective contact of silicon solar cells

Martin Bivour[a]*, Bart Macco[b], Jan Temmler[a], W. M. M. (Erwin) Kessels[b], Martin Hermle[a]

[a]*Fraunhofer Institute for Solar Energy Systems ISE, Heidenhofstrasse 2, 79110 Freiburg, Germany,*
[b]*Department of Applied Physics, Eindhoven University of Technology, P.O. Box 513, 5600 MB Eindhoven*

Abstract

Passivating and carrier selective contacts formed by metal oxide induced junctions are promising candidates to improve the efficiency of silicon solar cell. Important aspects for the optimization of such induced junctions are addressed by means of numerical device simulations. Experimentally, atomic layer deposited (ALD) molybdenum oxide (MoO_x) films are tested for their ability to form a hole-selective contact. To this end, the induced c-Si band bending, the external and implied V_{oc} and the crystallinity of the films are analyzed. It is shown that the properties of the induced p/n-junction are strongly influenced by the deposition temperature and the type of buffer layer applied. While a clear correlation between the induced band bending and the external V_{oc} is observed, the overall level remains well below that of a reference system for which thermally evaporated MoO_x was used. These results indicate that for the investigated ALD films a too low work function is limiting the formation of an efficient hole contact.

Peer review by the scientific conference committee of SiliconPV 2016 under responsibility of PSE AG.

Keywords: molybdenum oxide; work function; induced junction; silicon heterojunction

* Corresponding author. Tel.: +49 761/4588-5586
E-mail address: Martin.Bivour@ise.fraunhofer.de

Peer review by the scientific conference committee of SiliconPV 2016 under responsibility of PSE AG.
doi:10.1016/j.egypro.2016.07.125

1. Introduction

The application of adequate high and low work function (WF) contact materials for the formation of the hole and electron selective contacts, respectively, is well known from conductor–insulator-semiconductor (e.g. MIS) systems [1]. The WF difference of the heterojunction formed between the contact material and the absorber induces a band bending into the absorber which leads to the formation of an induced homojunction. If properly designed, the rectifying behavior is similar to a junction formed by n- or p-type doping of the absorber surface but the overall voltage level can be higher. The latter is explained by the fact that the layer (stack) placed on top of the c-Si absorber can not only provide a selective excess carrier extraction from the absorber but also good chemical passivation of the c-Si surface and a low recombination in the layer (stack) itself. Furthermore, the detrimental influence of very high carrier densities in the contact region, i.e. heavy doping effects like Auger recombination and band gap narrowing (BGN) is expected to be of minor importance.

With respect to high WF contact materials, the applicability of transition metal oxides adopted from organic electronics [2], [3] was invested for silicon thin film [4], [5] and more recently for c-Si absorbers [6], [7]. Thermally evaporated molybdenum oxide (MoO_x), a material already proposed back in 1980 [8], revealed to be an interesting candidate to replace the p-type a-Si:H. However, while MoO_x can outperform a-Si:H(p) in the as-deposited state [7], a crucial challenge is the formation of a hole barrier during low temperature annealing adversely affecting the *FF* and even the V_{oc} [7], [9]. So far, the exact nature of this problem is not fully understood. In general, a more holistic understanding of the relevant MoO_x / c-Si heterojunction properties is essential for an effective junction engineering.

As an alternative to thermally evaporated films, MoO_x formed by plasma enhanced atomic layer deposition (PE-ALD) [10], [11], [12] is investigated here. This is motivated by the facts that ALD might allow for a wide control over the material properties and that (spatial) ALD is an interesting approach for the industrial deposition of ultra-thin films [13]. While first investigations on device level [12] indicated that such films might not be suited, this paper is aiming for a more detailed investigation to assess the selective hole extraction. To this end the induced c-Si band bending, surface passivation and the external V_{oc} of solar cell-like test structures are probed for a range of MoO_x deposition temperatures. These electrical investigations are supplemented by Raman measurements. Furthermore, important aspects of such induced junctions are addressed by device simulations.

2. Simulation

2.1. Basic requirements on induced junctions

A simple metal-semiconductor like contact is simulated with AFORS-HET [14] to motivate the basic requirements of such passivating and carrier selective contact schemes based on an induced junction. By doing so the properties of the actual ITO / MoO_x / a-Si:H(i) / c-Si(n) heterojunction (Fig. 1,right) are reduced to the WF of a metal like contact layer and the chemical surface passivation provided by the stack. While the WF was changed from the conduction band energy to the valence band energy of the c-Si absorber, three different surface recombination velocities (S_0) were assumed to demonstrate the influence of the chemical c-Si passivation. The results for a hole (green) and electron contact (grey) are presented in Fig. 1, left. However, only the hole contact will be addressed in this work. For more details the reader is referred to Ref. [15], [16].

The importance of a sufficiently high WF to induce a band bending ($\varphi_{c\text{-}Si}$) and p/n-junction with an equilibrium hole density (p_0) similar to that of a junction formed by doping can be derived from the upper graph. For a WF close to the valence band the n-type absorber is highly inverted ($p_0 >> n_0$). The increase of the WF directly translates in a likewise increase of $\varphi_{c\text{-}Si}$, meaning the slope of $\varphi_{c\text{-}Si}$ is unity over the whole range. The implied voltage (i*V*) and external voltage (*V*) for open-circuit and maximum-power-point conditions are shown in the graphs below. The upper limit of the extractable voltage is given by the i*V* for all cases. It is defined by the interplay between excess carrier generation and recombination in the bulk and at the surface of the absorber. A high WF close to the valence band ensures that $p >> n \approx \Delta n$, i.e. low-injection conditions, are maintained in the contact region during operation which is the basic requirement to fully extract this voltage at the external electrodes. For such conditions the gradient of the majority carrier quasi Fermi-level in the contact region is negligible [17] and the external *V* matches

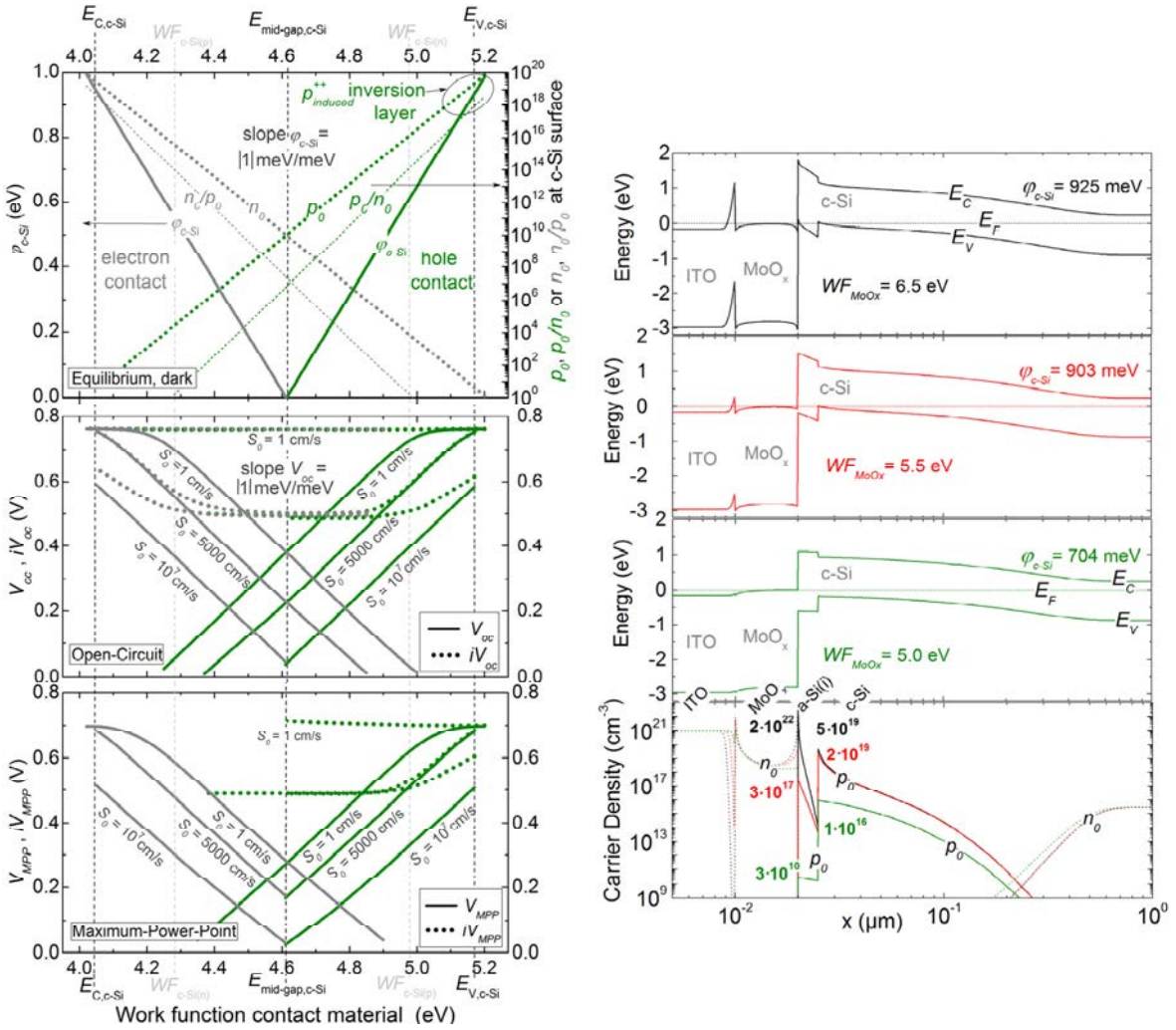

Fig. 1: Left, simulation results for a metal-semiconductor like contact system showing the influence of the contact layer work function and the chemical c-Si passivation on the properties of an induced p/n-junction. In green and grey the results for a hole contact of a n-type absorber and the electron contact of a p-type absorber, respectively. Right, possible equilibrium band diagrams and carrier densities for the experimentally investigated structure obtained with wxAMPS [18]. Numbers in the lower graph correspond to the induced equilibrium hole density at the MoO_x / a-Si:H(i) and the a-Si:H(i) / c-Si interface.

i*V*. Hence, excess carrier and voltage extraction can be regarded as ideal. While a better surface passivation improves the excess carrier density in the absorber and thus the overall voltage level. The higher excess carrier density comes along with greater demands on the WF. A higher induced p_0 is needed to ensure that $p >> n$ in the contact region remains fulfilled for all working conditions. Additionally, by comparing the middle and lower graph, it becomes apparent that maintaining $V = iV$ is more crucial for MPP compared to open-circuit conditions. Basically, since Fermi-level pinning and other (adjacent) junctions than the induced p/n-junction are not considered here, the slope of the external voltage is defined by the induced band bending. Hence, it is also unity until the limitation of implied voltage by the intrinsic bulk recombination of the absorber is reached (~755 mV for open-circuit).

For some qualitative consideration on the more heterojunction specific aspect of the experimentally investigated structures, the equilibrium band diagram and carrier densities of the ITO / MoO_x / a-Si:H(i) / c-Si(n) structure are

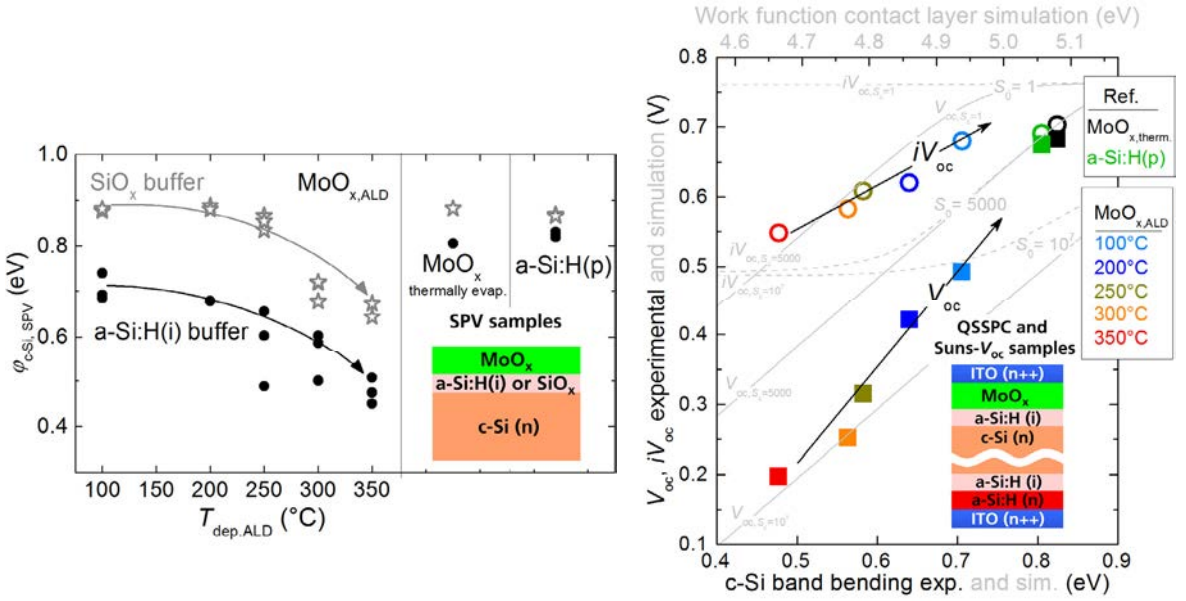

Fig. 2: Left, c-Si band bending as a function of the ALD deposition temperature for MoO_x films on a-Si:H or SiO_x buffer layers. Results for a thermally evaporated MoO_x and a-Si:H(p) reference are also shown. Right, external V_{oc} and implied V_{oc} as a function of the c-Si band bending, arrows are a guide to the eye. The grey lines correspond to results from numerical device simulations for the three different levels of chemical surface passivation, taken from Fig. 1. Inside the graphs, sketch of device structures used to determine the induced c-Si band bending (left) and the implied and external V_{oc} (right).

shown in Fig. 1,right. Three different WF values were assumed for the high band gap n-type MoO_x by modifying only the electron affinity of the layers. The WF of the high band gap degenerated n-type ITO is fixed to about 4.7 eV. As shown above, an decrease of the MoO_x WF decreases $\varphi_{c\text{-}Si}$ and hence p_0 in the a-Si:H(i) / c-Si(n) contact region. Further on, the overlap of the valence band of the a-Si:H(i) buffer and the conduction band of the MoO_x vanishes. Accordingly, besides a reduction of p_0 a carrier transport based on band-to-band tunnelling at the MoO_x / a-Si:H(i) junction might also be adversely affected by a low WF of MoO_x hampering the hole extraction. For such conditions an efficient tunnelling recombination junction must be formed by the contact to enable an efficient transport. The latter also being strongly influence by the defects of the films involved. It should be noted that these problems shows some affinity to the ITO / doped a-Si:H contact discussed in Ref. [19]. Another possible barrier for which the actual influence is hardly investigated is the conduction band offset at the ITO / MoO_x junction and the induced junction which results from the (significant) WF difference between both materials. A further variable not shown here is a very low electron density in the MoO_x layer. It could limit the conductivity of the MoO_x films and adjacent layers can easily modify the Fermi-level / carrier density within the MoO_x. The latter should be a problem especially if the MoO_x is thinner than its effective screening length. Aiming for a more holistic view, further work is needed to shed light on such issues.

3. Experimental

About 10 nm thick MoO_x films were deposited by a plasma assisted ALD process using $(NtBu)_2(NMe_2)_2Mo$ as Mo precursor and O_2 plasma as oxidant in a Oxford Instruments OpAL system. Mo precursor dosing was done by bubbling, using 50 sccm of Ar as carrier gas. The Mo precursor bubbler was held at 50 °C, and the delivery lines were heated to 60 °C to avoid condensation of the precursor. The table temperature ($T_{dep.ALD}$) is the reported temperature and was varied between 100 and 350 °C. The chamber walls are heated to the table temperature, with a

maximum of 180 °C. The Mo precursor dose and purge times are 6 and 3 s, respectively. The O_2 plasma step took 4 s with 50 sccm O_2 and a plasma power (ICP) of 100 W followed by a purge of 5 s. Thermally evaporated MoO_x (non-reactive, no intentional heating) and a-Si:H(p) were used as reference. Further details on the samples preparation and the measurement setups can be found elsewhere [20], [7], [11].

3.1. Induced c-Si band bending

To probe the induced c-Si band bending surface photo-voltage (SPV) measurements were performed on structures featuring either an wet chemically grown SiO_x buffer layer or an a-Si:H(i) buffer as indicated in Fig. 2 Fig. 2: Left, c-Si band bending as a function of the ALD deposition temperature for MoO_x films on a-Si:H or SiO_x buffer layers. Results for a thermally evaporated MoO_x and a-Si:H(p) reference are also shown. Right, external V_{oc} and implied V_{oc} as a function of the c-Si band bending, arrows are a guide to the eye. The grey lines correspond to results from numerical device simulations for the three different levels of chemical surface passivation, taken from (SPV samples).

The left graph in Fig. 2 reveals that $\varphi_{c\text{-}Si}$ is reduced for higher $T_{dep.ALD}$ and that the induced band bending is much higher for samples with the SiO_x buffer. The latter might be explained by the fact that Fermi-level pinning is less pronounced for the SiO_x buffer, that some band bending is lost in the a-Si:H buffer or that the type of buffer / substrate is influencing the actual film grows and properties. While a final statement cannot be given here, according to simulation results (not show) it is unlikely that 200 meV are lost in the about 7 nm thick a-Si:H buffer. Regarding Fermi-level pinning, at least for metal contact layer a less pronounced pinning is observed for SiO_x [21] compared to a-Si:H [22], [16], [23]. For the a-Si:H buffer the maximum $\varphi_{c\text{-}Si}$ remains about 100 meV below the references. Considering the close dependence of the external voltage on the WF and hence $\varphi_{c\text{-}Si}$ from Fig. 1,left a significant voltage loss and a non-ideal carrier extraction are expected for the ALD films combined with an a-Si:H buffer.

3.2. Voltage extraction and surface passivation

The films were also investigated with the solar cell like test structures in Fig. 2 (QSPPC and Suns-V_{oc} samples). The iV_{oc} and the external V_{oc} near 1 sun conditions was analyzed to evaluate whether the external V_{oc} is limited by surface passivation or a non-ideal voltage extraction. Both parameters are plotted in the right graph in Fig. 2 as function of $\varphi_{c\text{-}Si}$ determined in the previous subsection. The grey lines serve as a guide to the eye and are taken from the simulation results in Fig. 1. A detailed investigation of structures featuring the SiO_x buffer was not performed due to the absence of surface passivation.

A clear correlation between $\varphi_{c\text{-}Si}$ and the V_{oc} is observed. However, the V_{oc} remains well below that of the references. That these low V_{oc}s are limited by a poor carrier selectivity rather than surface passivation can be followed from two facts. Firstly, the gap between the iV_{oc} and the V_{oc} is significant and increased for lower $\varphi_{c\text{-}Si}$. Secondly, a V_{oc} well below 600 meV can only be reached if a poor carrier selectivity is involved. This becomes obvious considering the simulation results. For a highly inverted c-Si surface ($\varphi_{c\text{-}Si} > 0.8$ eV) without any chemical surface passivation ($S_0 = 10^7$ cm/s) the V_{oc} predicted by the simulations remains well above the 200 - 500 mV obtained for the ALD MoO_x films. Regarding the iV_{oc}, the drop for lower $\varphi_{c\text{-}Si}$ will partly be caused by a reduced field-effect passivation, due to the lower inversion of the c-Si surface. But a thermal degradation of the chemical surface passivation by the a-Si:H buffer for $T_{dep.ALD} \geq 200$°C is also very likely. The results above suggest that the WF of MoO_x is significantly influenced by $T_{dep.ALD}$ and increases for lower $T_{dep.ALD}$. The fact that the $\varphi_{c\text{-}Si}$ remains well below that of the references is pointing towards a too low WF of the ALD MoO_x films which is limiting the selective extraction of excess holes from the absorber.

It should be noted that other investigations like annealing the samples, omitting the a-Si:H buffer, using a thinner a-Si:H buffer, replacing the ITO by a metal and decreasing the MoO_x thickness have also been conducted. However, without significantly affecting the limitation of the external voltage by an insufficient carrier selectivity.

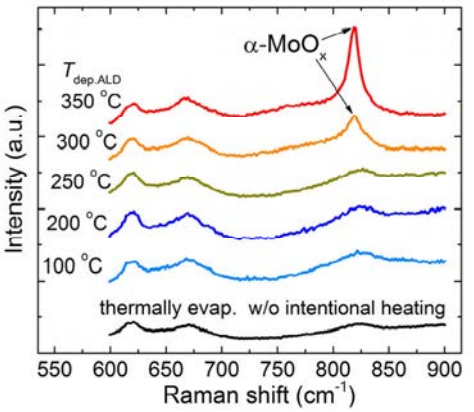

Fig. 3: Raman spectra of the MoO_x films deposited at temperatures between 100 and 350 °C.

3.3. Crystallinity

To link the electric properties from above with the films properties, the crystallinity of the different layers has been determined by Raman spectroscopy. The results in Fig. 3 reveal that the crystallinity of the ALD films increases with $T_{dep.ALD}$. A pronounced peak around 818 cm^{-1} for above 250°C is visible indicating the films are in the stable orthorhombic α-phase. The absence of such peaks for films deposited at lower temperatures and the thermally evaporated films indicates their amorphous nature which is in line with the results from Ref. [11]. The results suggest that amorphous MoO_x is preferred, possibly due to a higher WF of such films. However, for a final statement further investigations are needed to link the poor carrier selectivity obtained for the ALD films with their material properties. This includes detailed investigations of the chemical and structural MoO_x properties and a comparison with the well performing evaporated films.

4. Summary

Important aspects for the optimization of passivating and carrier selective contacts based on induced junction were addressed by means of numerical device simulations. Their close affinity to the well-known conductor-insulator-semiconductor system was stressed. Experimentally, a variation of the deposition temperature of plasma assisted ALD deposited MoO_x revealed to have a strong influence on the properties of a hole selective contact formed by such films. In accordance with simulations, a clear correlation between the induced c-Si band bending and the external V_{oc} was observed. While both are increased for lower deposition temperatures, the induced band bending and hence the V_{oc} remain well below the level obtained for films deposited by thermal evaporation. It could be shown that the low V_{oc} is limited by poor carrier selectivity, most likely caused by a too low work function of the ALD MoO_x, rather than an insufficient surface passivation. Raman measurements revealed that the film crystallinity is also influenced by the deposition temperature and that better carrier selectivity and higher V_{oc}s are obtained for amorphous films. The presented investigations pointed out that that further optimization of the ALD films is needed to form an efficient hole contact. This includes structural investigations to link the crystallinity and other films properties like the chemical composition / stoichiometry with e.g. the work function and the obtained carrier selectivity.

Acknowledgements

The colleagues at ISE are acknowledged for the experimental / technical assistance and Frank Feldmann for fruitful discussions. This work was funded by the German Federal Ministry for the Economy and Energy under grant No. 0325292”ForTeS”. B.M. acknowledges STW (Stichting Wetenschap en Technologie) for financial support.

References

[1] R. Singh, M. A. Green and K. Rajkanan, Review of conductor-insulator-semiconductor (CIS) solar cells, Solar Cells 1981; 3 95-148.
[2] S. Chen, J. R. Manders, S.-W. Tsang, et al., Metal oxides for interface engineering in polymer solar cells, Journal of Materials Chemistry 2012; 22 24202–24212.
[3] M. T. Greiner and Z.-H. Lu, Thin-film metal oxides in organic semiconductor devices: their electronic structures, work functions and interfaces, NPG Asia Mater 2013; 5 e55.
[4] S. Il Park, S. Jae Baik, J.-S. Im, et al., Towards a high efficiency amorphous silicon solar cell using molybdenum oxide as a window layer instead of conventional p-type amorphous silicon carbide, Applied Physics Letters 2011; 99 063504.
[5] L. Fang, S. J. Baik, J. W. Kim, et al., Tunable work function of a WOx buffer layer for enhanced photocarrier collection of pin-type amorphous silicon solar cells, Journal of Applied Physics 2011; 109 104501.
[6] C. Battaglia, X. Yin, M. Zheng, et al., Hole selective MoOx contact for silicon solar cells, Nano letters 2014.
[7] M. Bivour, J. Temmler, H. Steinkemper, et al., Molybdenum and Tungsten Oxide: High Work Function Wide Band Gap Contact Materials for Hole Selective Contacts of Silicon Solar Cells, Solar Energy Materials and Solar Cells 2015; 34–41.
[8] J. Shewchun, D. Burk and M. B. Spitzer, MIS and SIS solar cells, Electron Devices, IEEE Transactions on 1980; 27 705-716.
[9] J. Geissbühler, J. Werner, S. Martin de Nicolas, et al., 22.5% efficient silicon heterojunction solar cell with molybdenum oxide hole collector, Applied Physics Letters 2015; 107 081601.
[10] B. Macco, M. F. J. Vos, N. F. W. Thissen, et al., Low-temperature atomic layer deposition of MoOx for silicon heterojunction solar cells, physica status solidi (RRL) – Rapid Research Letters 2015.
[11] M. F. J. Vos, B. Macco, N. F. W. Thissen, et al., Atomic layer deposition of molybdenum oxide from (NtBu)2(NMe2)2Mo and O2 plasma, Journal of Vacuum Science & Technology A 2016; 34 01A103.
[12] J. Ziegler, M. Mews, K. Kaufmann, et al., Plasma-enhanced atomic-layer-deposited MoO x emitters for silicon heterojunction solar cells, Applied Physics A 2015; 1-6.
[13] P. Poodt, D. C. Cameron, E. Dickey, et al., Spatial atomic layer deposition: A route towards further industrialization of atomic layer deposition, Journal of Vacuum Science & Technology A 2012; 30 010802.
[14] R. Varache, C. Leendertz, M. E. Gueunier-Farret, et al., Investigation of selective junctions using a newly developed tunnel current model for solar cell applications, Solar Energy Materials and Solar Cells 2015; 141 14-23.
[15] M. Bivour, M. Reusch, F. Feldmann, et al., Requirements for Carrier Selective Silicon Heterojunctions, in 24th Workshop on Crystalline Silicon Solar Cells & Modules: Materials and Processes, Breckenridge, Colorado, 2014.
[16] M. Bivour, Silicon heterjunction solar cells: Analysis and basic unterstanding, PhD thesis, University Freiburg, 2016 in press.
[17] P. Würfel, Physics of Solar Cells - From principles to new concepts. Weinheim: Wiley-Vch Verlag GmbH & Co KgaA, 2005.
[18] Y. Liu, Y. Sun and A. Rockett, A new simulation software of solar cells—wxAMPS, Solar Energy Materials and Solar Cells 2012; 98 124-128.
[19] A. Kanevce and W. K. Metzger, The role of amorphous silicon and tunneling in heterojunction with intrinsic thin layer (HIT) solar cells, Journal of Applied Physics 2009; 105 094507-1--094507-7.
[20] M. Bivour, M. Reusch, S. Schroer, et al., Doped Layer Optimization for Silicon Heterojunctions by Injection-Level Dependent Open-Circuit Voltage Measurements, IEEE Journal of Photovoltaics 2014; 566-574.
[21] Y.-C. Yeo, T.-J. King and C. Hu, Metal-dielectric band alignment and its implications for metal gate complementary metal-oxide-semiconductor technology, Journal of Applied Physics 2002; 92 7266.
[22] C. R. Wronski and D. E. Carlson, Surface states and barrier heights of metal-amorphous silicon schottky barriers, Solid State Communications 1977; 23 421-424.
[23] K.-U. Ritzau, M. Bivour, S. Schröer, et al., TCO work function related transport losses at the a-Si:H/TCO-contact in SHJ solar cells, Solar Energy Materials and Solar Cells 2014; 131 9-13.